Experimental Physiology

Identification of arterial wall dynamics in conscious dogs

Lucas G. Gamero *†, Ricardo L. Armentano *§, Juan G. Barra *, Alain Simon ‡ and Jaime Levenson ‡

* *Favaloro University, Solís 453, (1078) Buenos Aires,* † *Facultad de Ingeniería, Universidad Nacional de Entre Ríos y Universidad de Buenos Aires, Buenos Aires, Argentina and* ‡ *Cardiovascular, CRI (INSERM) Hôpital Broussais, 96 rue Didot, Paris 14, France*

(Manuscript received 17 November 2000; accepted 17 April 2001)

Viscoelastic properties determine the dynamic behaviour of the arterial wall under pulsatile pressure and flow, suggesting time- or frequency-dependent responses to changes in wall stress and strain. The objectives of the present study were: (i) to develop a simplified model to derive simultaneously the elastic, viscous and inertial wall moduli; (ii) to assess Young's modulus as a function of frequency, in conscious, chronically instrumented dogs. Parametric discrete time models were used to characterise the dynamics of the arterial system based on thoracic aortic pressure (microtransducer) and diameter (sonomicrometry) measurements in control steady state and during activation of smooth muscle with the α-adrenoceptor agonist phenylephrine (5 μg kg^{-1} min^{-1}, I.V.), in eight conscious dogs. The linear autoregressive model and a physically motivated non-linear model were fitted to the input–output (stress–strain) relationship. The aortic buffering function (complex Young's modulus) was obtained *in vivo* from the identified linear model. Elastic, viscous and inertial moduli were significantly increased from control state ($(44.5 \pm 7.7) \times 10^4$ Pa; $(12.3 \pm 4.7) \times 10^4$ Pa s; $(0.048 \pm 0.028) \times 10^4$ Pa s^2) to active state ($(85.3 \pm 29.5) \times 10^4$ Pa, $P < 0.001$; $(22.4 \pm 8.3) \times 10^4$ Pa s, $P < 0.05$; $(0.148 \pm 0.060) \times 10^4$ Pa s^2, $P < 0.05$). These moduli, obtained using the linear model, did not present significant differences compared with those derived using the non-linear model. In control conditions, the magnitude of the normalised complex Young's modulus was found to be similar to that reported in previous animal studies ranging from 1 to 10 Hz. During vascular smooth muscle activation, this modulus was found to be increased with regard to control conditions ($P < 0.01$) in the frequency range used in this study. The frequency-dependent Young's modulus of the aortic wall was obtained for the first time in conscious, unsedated dogs. The parametric modelling approach allows us to verify that vascular smooth muscle activation increases the elastic, viscous and inertial moduli with the advantage of being able to track their time evolution. Furthermore, under activation, the aortic wall remains stiff in the physiological frequency range, suggesting the impairment of the arterial buffering function. *Experimental Physiology* (2001) **86.4**, 519–528.

Today, there is a growing interest in the physical properties of large arteries. Hence, an accurate characterisation of the behaviour of these arteries could contribute to a better understanding of the material and underlying dynamics. Viscoelastic properties of the arterial wall determine the response to dynamic forces such as pulsatile pressure and flow (Milnor, 1982; Nichols & O'Rourke, 1990; Simon *et al.* 1991) and hence potentially cellular/molecular biological responses (Davies, 1995). The presence of viscous components in the arterial wall suggests time- or frequency-dependent responses to changes in wall stress (Peterson *et al.* 1960; Bergel, 1961; Milnor, 1982; Nichols & O'Rourke, 1990). The dynamic behaviour of arteries at different frequencies is an important element in both theoretical and practical haemodynamics. When the Young's modulus of the arterial wall is determined as a function of frequency, a particular behaviour is found. For frequencies from 0.01 to 1.5 Hz, the amplitude of the complex Young's modulus rises steeply to a quite constant level (Fung, 1981; Cox, 1984). This value is reached at frequencies below heart rate. Hardung (1970) and Goedhard *et al.* (1973) have provided data in this low frequency range from *in vitro* experiments. Sipkema (1979) studied the viscoelastic behaviour by means of a servo-controlled occluder system *in vivo*. Gow & Taylor (1968) measured the viscoelastic properties of arteries in anaesthetised animals in both the low and the high frequency ranges using power spectrum analysis from pressure and diameter data. The power spectrum method provides frequency–response information, but it does not consider explicitly mechanical properties of the arterial wall. Moreover, tracking of time-varying dynamic properties is also difficult using a non-parametric transfer function estimation method.

§ Corresponding author: armen@favaloro.edu.ar

On the other hand, smooth muscle cells, dominantly responsible for wall viscosity, constitute one of the main determinants of the dynamic behaviour of the arterial wall. It must be pointed out that dynamic studies of large arteries involving vascular smooth muscle (VSM) activation are difficult to carry out in anaesthetised animals (Dobrin, 1984).

Several constitutive models describing arterial wall behaviour were developed with the aim of estimating the physiological parameters that mainly influence circulatory mechanics (Westerhof & Noodergraaf, 1970; Fung, 1981; Langewouters *et al.* 1984; Hayashi, 1993; Armentano *et al.* 1995*a*; Wuyts *et al.* 1995). Most of these models spring from simple anatomophysiological considerations such as incompressibility, isotropy and linear elastic behaviour of the aortic wall. Our group (Armentano *et al.* 1995*a*) developed a complete constitutive model description of the arterial wall taking into account three main mechanical properties: elasticity, viscosity and inertia. A sequential and iterative procedure was proposed to estimate the model parameters. However, this procedure lacks the possibility of obtaining estimates in real time and of computing the frequency response due to the non-linear elasticity.

System identification is a well-established methodology and concerns the problem of designing mathematical models of dynamical systems based on observed data. For these purposes, a new method is presented, considering the arterial wall as a dynamic system. We built a semiphysical physiologically motivated model structure and the parameters were computed using a system identification approach. To overcome the problems described above, a parametric modelling and identification procedure for simultaneous assessment of the viscoelastic properties and the frequency response behaviour is proposed in the present study. This procedure involves two important steps: modelling and parameter estimation (system identification). To solve the problem of real time identification, recursive algorithms are employed.

Our main objectives were: first, to derive simultaneously through the models the constitutive parameters that best represent the system controlling the arterial wall dynamics; and second, to obtain the frequency dependence of Young's modulus from the identified model in order to characterise the aortic buffering function and its behaviour under VSM activation in chronically instrumented conscious dogs.

METHODS

Surgical preparation

Eight male mongrel dogs aged 4.9 ± 1.9 years and weighing 22.2 ± 2.9 kg were prepared for this study. On arrival to the animal house, the dogs were vaccinated against common canine diseases and were treated for skin and intestinal parasites. During the 20 days before surgery they were appropriately fed and watered and assessed for adequate clinical status.

Anaesthesia was induced with intravenous thiopental sodium (20 mg kg^{-1}) and, after intubation, maintained with 2% enflurane carried in pure oxygen (4 l min^{-1}) through a Bain tube connected to a Bird Mark VIII respirator. A sterile thoracotomy was made at the left fifth intercostal space. A pressure microtransducer (Konigsberg P7) and a fluid-filled polyvinyl chloride catheter (2.8 mm o.d.) for later calibration of the microtransducer were implanted in the descending thoracic aorta through an incision in the left brachial artery. A pair of ultrasonic crystals (5 MHz, 4 mm diameter) was sutured on the adventitia of the aorta, after minimal dissection, to measure external aortic diameter. The transit time of the ultrasonic signal (1580 m s^{-1}) was converted into distance using a sonomicrometer (Triton Technology Inc.) and observed on the screen of an oscilloscope (Tektronix 465B) to confirm optimal signal quality. A polyvinyl chloride catheter (2.3 mm o.d.) was advanced through the left mammary vein to lie in the superior vena cava or right atrium for drug administration.

Before repairing the thoracotomy, all cables and catheters were tunnelled subcutaneously to emerge at the interscapular space. All animals were allowed to recover under veterinary care. Ampicillin (20 mg kg^{-1} day^{-1}, per os) was given for 7 days after surgery. The catheters were flushed daily with heparinised saline. The experiments were performed in accordance with the *Guide for the Care and Use of Laboratory Animals* published by the US National Institutes of Health (NIH Publication no. 85-23, revised 1996).

Experimental protocol

Experiments were performed starting on the seventh postoperative day. Each study was performed with the dog resting quietly on its right side in the conscious, unsedated state. The aortic pressure was measured using the pressure microtransducer, which had been calibrated against a Statham-P23 transducer connected to the aortic fluid-filled catheter. The zero reference point was set at the level of the right atrium. Instantaneous pressure–diameter loops were displayed on-line and stored on a computer (PC Pentium 200 MHz MMX using an analog–digital converter card (National Instruments Lab-PC. Sample frequency was set at 200 Hz. A 5% dextrose drip (0.25 ml min^{-1}) was started through the mammary vein catheter. Each steady state comprised the recording of aortic pressure and external diameter under control conditions and during administration of phenylephrine (5 μg kg^{-1} min^{-1}) infused in parallel with the dextrose drip.

After a period in the control state, VSM was activated by infusion of phenylephrine. The instantaneous pressure–diameter loops were monitored until stabilisation was achieved. We waited 15–20 min to ensure a steady state under phenylephrine infusion, and confirmed by visual inspection that the pressure–diameter loops shifted towards a higher pressure level with respect to control conditions. Two days later, the dogs were killed with an overdose of thiopental sodium followed by potassium chloride. The correct positioning of the dimension gauges in all dogs was verified at necropsy.

Data collection

Approximately 20 consecutive beats during basal conditions and during activation of VSM were averaged to obtain mean, systolic, diastolic and pulse aortic pressures and diameter, and heart rate. Diastolic onset was detected by analysing the first derivative of the pressure waveform as can be seen in Fig. 1. We considered diastolic onset as the maximum value of pressure between the first local maximum following the negative peak of the derivative (point A) and the onset of the rapid upstroke of the derivative of aortic pressure (point B).

The procedure to determine the aortic dynamic behaviour was developed in our laboratory under Matlab (The Mathworks, Inc., MA, USA). Aortic wall thickness was calculated as the

difference between the external aortic radius r_e and the internal aortic radius r_i. To estimate r_i we used a procedure that assumes the non-variability of the wall volume (Dobrin & Rovick, 1969; Armentano *et al.* 1995*a*). Strain e was obtained from the ratio of midwall radius

$$R = (r_e + r_i)/2$$

to the non-stressed midwall radius R_0 measured approximately at 25 mmHg of aortic pressure (Armentano *et al.* 1995*a*) during necropsy:

$$\epsilon = R/R_0.$$

Stress σ was assessed using a linear elastic theory and assuming an isotropic, homogeneous elastic material for the aortic wall (Pagani *et al.* 1979; Vatner *et al.* 1984)

$$\sigma = \frac{2P(r_e\, r_i)^2}{r_e^2 - r_1^2}\frac{1}{R^2},$$

where P is aortic pressure.

System modelling and identification

The problem of identifying a mathematical model of an unknown system from a sequence of empirical data is a fundamental one, which arises in many branches of science and engineering. The complexity of solving such a problem depends on many factors, such as *a priori* knowledge, quality and completeness of the data sequence, and required model form and accuracy. After experiment design, the problem can be split into two parts: model structure selection and parameter estimation. Various least-squares types of algorithms are predominant for parameter estimation. There is a large spectrum of model structure approaches to choose among (Sugeno & Kang, 1988; Ljung, 1999). The aim of this study was to handle the given system using physical and physiological evidence about the system in order to solve the structure selection problem. In the next subsections, a theoretical background concerning the viscoelastic models as well as the basic tools of system identification are summarised.

Linear viscoelastic model

The continuous-time linear viscoelastic behaviour can be modelled by the following differential equation (Westerhof & Noordergraaf, 1970; Christensen, 1971):

$$\sum_{i=0}^{n} c_i\, \mathrm{d}^i\epsilon/\mathrm{d}t^i = \sum_{j=0}^{m} d_j\, \mathrm{d}^j\sigma/\mathrm{d}t^j, \qquad (1)$$

where ϵ is the strain and σ the stress. The coefficients $\{c_i, i = 1, ..., n\}$ and $\{d_j, j = 1, ..., m\}$ define the material's viscoelastic properties. The model order is represented by n and m. The description of the viscoelastic properties as represented in eqn (1) is general when the material is linear and time invariant or when only very small excursions from a working point are considered (Gow & Taylor, 1968). Since the arterial wall is not linear, we considered the measured data about a working point, which can be established to be around the mean arterial diameter and pressure measurements.

A frequency domain representation of the general model (eqn (1)) can be derived applying the Laplace transform. Then, the complex Young's modulus is given by:

$$E(j\omega) = \frac{\sum_{i=0}^{n} c_i (j\omega)^i}{1 + \sum_{j=1}^{m} d_j (j\omega)^j}. \qquad (2)$$

This equation allows us to compute the frequency response of the system given the coefficients c_i, and d_j and letting $s = j\omega$.

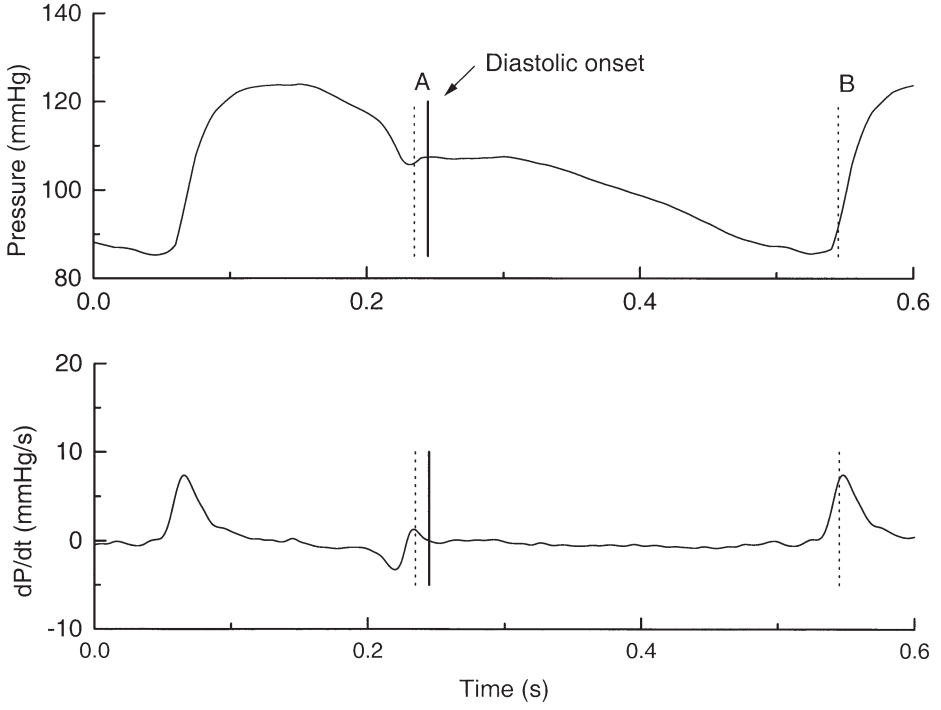

Figure 1

Definition of diastolic onset computed by means of pressure waveform and its first derivative.

Table 1. Steady state basal haemodynamic parameters in control and during infusion of phenylephrine

	Control (n = 8)	Activation (n = 8)
Aortic systolic pressure (mmHg)	124.9 ± 9.9	193.0 ± 15.4 *
Aortic diastolic pressure (mmHg)	73.1 ± 9.1	126.1 ± 6.2 *
Aortic mean pressure (mmHg)	97.1 ± 8.1	156.5 ± 10.3 *
Aortic systolic diameter (mm)	17.29 ± 1.45	17.62 ± 1.39 *
Aortic diastolic diameter (mm)	15.54 ± 1.41	16.37 ± 1.28 *
Aortic mean diameter (mm)	16.52 ± 1.40	17.07 ± 1.33 ‡
Heart rate (beats min^{-1})	112.7 ± 19.5	104.3 ± 23.8

Values are means ± S.D. * $P < 0.02$, ‡ $P < 0.005$ (paired t test with respect to control condition in the 8 dogs in which phenylephrine infusion was made).

The problem of parameter estimation was investigated in the discrete time domain by means of on-line adaptive algorithms. Different discrete time structures were used for the identification purpose. We employed a single-input, single-output system and chose the stress as input and the strain as output. The linear autoregressive with exogenous input (ARX) model and the physically motivated non-linear NARX model (see Appendix) were fitted to each of the eight dogs during both control and conditions of VSM activation to assess the dynamics of the arterial system. The parameters for each model fit were estimated using the recursive least-squares algorithm, which provides an on-line adaptive structure method to track time-varying changes (see Appendix). For each model structure, the optimal model defined as that which minimised the Akaike information criterion (AIC) was chosen (see Appendix). Because estimation of the ARX and NARX models can quickly become computationally very expensive, a subset of model structures was selected. The maximum model order was set to 10. The results of this procedure gave us the best model order for each case considered. Such optimisation procedure is presented in Fig. 2, where a set of models were evaluated and the AIC was plotted as a function of the number of model parameters. Mean and standard error measures computed over the whole population are presented. Note that beyond $n = m = 3$ no differences were found in the fitness performance. The general third order model ($n = m = 3$) was chosen as the mean best order model. For the non-linear NARX case, a second order polynomial was obtained using the same procedure. A high order polynomial did not improve the model performance. After parameter estimation, the inverse bilinear transformation was used as a mapping procedure to obtain the viscoelastic parameters from the identified discrete time model (see Appendix).

In order to compare with previous reports, the elastic, viscous and mass moduli can be estimated from the general model. Several authors considering pressure–strain and pressure–flow relationships used a second order ordinary differential equation (Peterson *et al.* 1960; Westerhof & Noordergraaf, 1970; Gow *et al.* 1974; Sipkema, 1979; Armentano *et al.* 1995*a*):

$$E\epsilon + \eta\left(\mathrm{d}\epsilon/\mathrm{d}t\right) + M(\mathrm{d}^2\epsilon/\mathrm{d}t^2) = \sigma(t), \qquad (3)$$

where E, η and M are the elastic, viscous and mass moduli, respectively. With the proposed analysis, these moduli can be derived as a special case of eqn (1), from the identified third order model.

Statistical analysis

All measurements and calculated values are expressed as means ± S.D. Linear regression was analysed using the recursive least squares algorithm. The presence of significant differences in the estimated parameters was assessed using Student's paired t test. The magnitude of the complex Young's modulus was

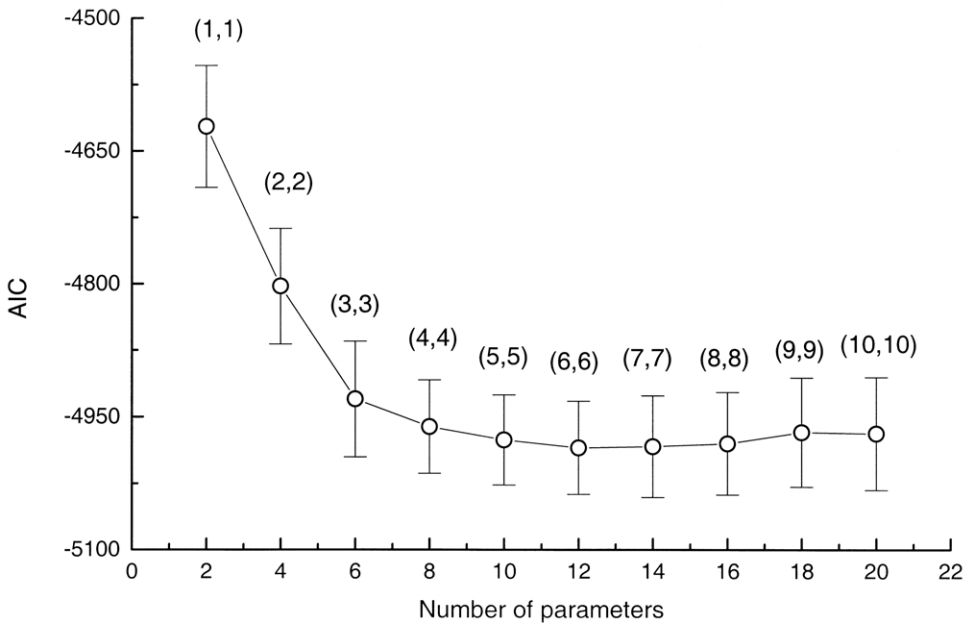

Figure 2

Linear model order estimation using Akaike information criterion (AIC) as a function of the total number of parameters considering general models with a maximum number of 20 parameters $\{n_x = 1, ..., 10\}$, $\{n_y = 1, ..., 10\}$. The data (○) are means ± S.E.M., computed over the whole population. The model order (n_x, n_y) is in parentheses.

analysed in each animal by measuring the area under the curve (AUC) within a frequency range 0–10 Hz. The AUC under smooth muscle activation was then compared with that corresponding to control conditions by using Student's paired *t* test. Values of $P < 0.05$ were considered statistically significant.

RESULTS

Dynamic wall parameters

Table 1 shows the haemodynamic parameters during control steady state and during phenylephrine activation of steady state VSM. Heart rate was the only variable that presented no statistical differences with respect to control conditions.

Local aortic system identification

The model fit during control and after the infusion of phenylephrine using the ARX general third order model of the eight data sets produced a mean residual variance (see Appendix) of $(6.14 \pm 3.17) \times 10^{-5}$ and $(4.80 \pm 1.47) \times 10^{-5}$, respectively. The corresponding NARX third order model with a second order polynomial modelling the pure elastic behaviour fits produced a mean residual variance of $(5.55 \pm 2.51) \times 10^{-5}$ during control and $(3.60 \pm 0.722) \times 10^{-5}$ in the active state.

Figure 3 shows the strain prediction using system identification by means of a general third order ARX model and a non-linear NARX model during control conditions. As can be seen, the estimated strain (thin and dotted lines) provides a good tracking of the true output (thick line) most of the time. The simulated linear model (thin line) presents a slight overshoot during the peak of the systolic phase compared with the measured strain. The NARX model considering a non-linear elastic behaviour provides a small improvement during the systolic phase (dotted line).

Table 2. Elastic (E, 10^4 Pa), viscous (η, 10^4 Pa s), inertial (M, 10^4 Pa s^2) moduli, estimated using the general third order ARX model structure and the NARX model with non-linear elastic behaviour

	E	η	M
Control ARX	44.5 ± 7.7	12.3 ± 4.7	0.048 ± 0.028
PHN ARX	85.3 ± 29.5 *	22.4 ± 8.3 ‡	0.148 ± 0.060 ‡
Control NARX	45.6 ± 12.8	10.4 ± 5.2	0.042 ± 0.032
PHN NARX	97.6 ± 44.0 ‡	24.4 ± 12.4 ‡	0.165 ± 0.105 ‡

Values are means ± S.D., * $P < 0.001$, ‡ $P < 0.05$, paired *t* test. No significant differences were obtained between the linear ARX and non-linear NARX model.

Arterial parameter estimation

Table 2 shows the main elastic parameters calculated from the entire population (8 dogs) assessed during control and VSM activation. The elastic, viscous and inertial moduli were computed from the discrete third order ARX models using the bilinear transformation. Using the linear part of the NARX model, the same viscoelastic parameters were derived (Table 2). The elastic, viscous and inertial moduli were increased significantly from control to the active state ($P < 0.05$). No significant differences were found comparing equivalent parameters between the linear ARX and non-linear NARX model.

Frequency response

The magnitude of the dynamic elastic modulus $|E(j\omega)|$ divided by a static value E_0 obtained from the identified model (see eqn (3) at $\omega = 0$), also known as the modulus ratio, was computed for each animal during both control and VSM

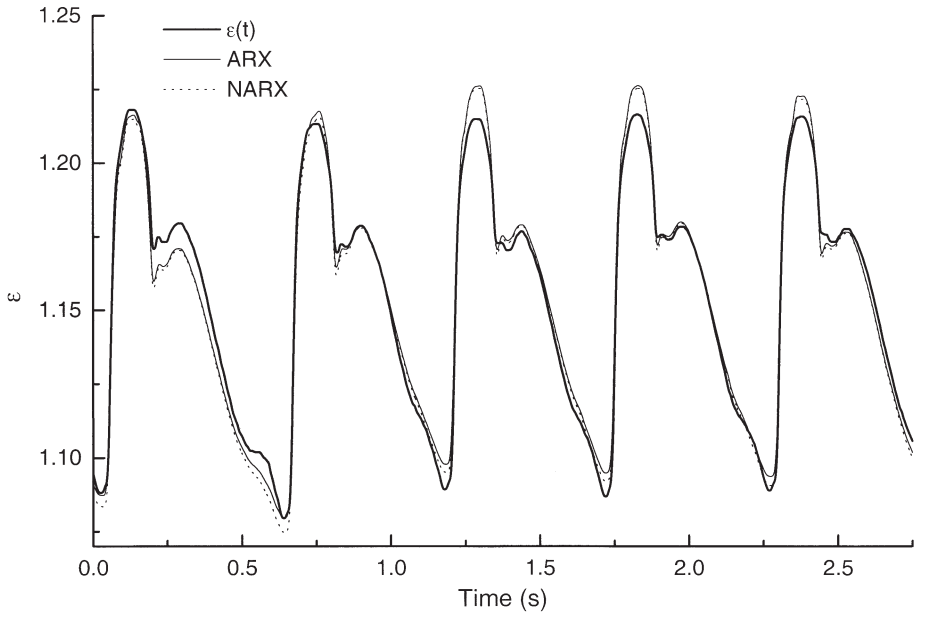

Figure 3

Results of the model fit (strain (ϵ) as a function of time) using the linear ARX (thin line) and non-linear NARX (dotted line) model approximations using validation (thick line) data during control.

activation and using the same ARX model order. Figure 4 summarises these results showing the mean values for the modulus ratio averaged over the entire population. The lowest part of the curve shows values obtained under conditions of low strain. There is an increase in the dynamic modulus from 0.02 to 1.5 Hz. Minimal changes occur between this value and frequencies up to 10 Hz. The magnitude of the normalised complex Young's modulus was significantly different ($P < 0.01$) from 1 to 10 Hz comparing control conditions and VSM activation.

Time-varying system modelling

In order to evaluate the parameters with the main influence on arterial dynamics, and their individual contribution, we applied the model proposed in eqn (1). The time evolution of the identified parameters was obtained using the adaptive identification procedure. During steady states the parameters do not present significant changes, as can be seen in Fig. 5. Figure 5*A* shows the time course of the measured strain. The elastic, viscous and inertial moduli as a function of time are presented in Fig. 5*B*, *C* and *D*, respectively. Beat-to-beat mean and standard deviation of the mechanical properties are also plotted.

DISCUSSION

The aim of this study was to obtain a complete characterisation of the arterial wall dynamics in conscious, unsedated, chronically instrumented dogs. A new method to characterise the *in vivo* regulation of aortic viscoelastic behaviour and the characteristic buffering function is presented. To our knowledge, no study regarding the assessment of the dynamic properties of the aortic wall using a system identification approach has been reported in conscious animals. To build the constitutive equation we proposed linear and non-linear general third order differential equations; the parameters derived from these models (the total elastic modulus, the viscous modulus and the inertial modulus) are physically meaningless. The total elastic modulus was assessed considering a linearised model at mean arterial pressure. To determine *in vivo* instantaneous pressure and diameter signals, ultrasonic dimension transducers and a miniature pressure gauge were used. This method, which has been validated in our laboratory (Cabrera Fischer *et al.* 1991; Barra *et al.* 1993), allows accurate and reproducible measurements (Milnor, 1982; Nichols & O'Rourke, 1990) over a long period of time (Dobrin & Rovick, 1969; Pagani *et al.* 1979). Aortic signals were converted into stress and strain using a thick-walled cylindrical tube model and linear elastic theory (Pagani *et al.* 1979; Fung, 1981). Stress was calculated instantaneously over the whole cardiac cycle (Dobrin & Rovick, 1969).

A constitutive non-linear differential equation previously reported by our group (Armentano *et al.* 1995*a*) considers the pure elastic, viscous and inertial behaviour using a sequential procedure developed to estimate the parameters of the constitutive equation. An iterative procedure of hysteresis elimination is used (Bauer, 1984; Barra *et al.* 1993; Armentano *et al.* 1995*a*) to determine the viscous behaviour of the arterial wall, and after that the inertial modulus is computed over the remaining hysteresis loop. Finally, the purely elastic contribution is computed using a non-linear fitting procedure. One drawback of this algorithm is that it is

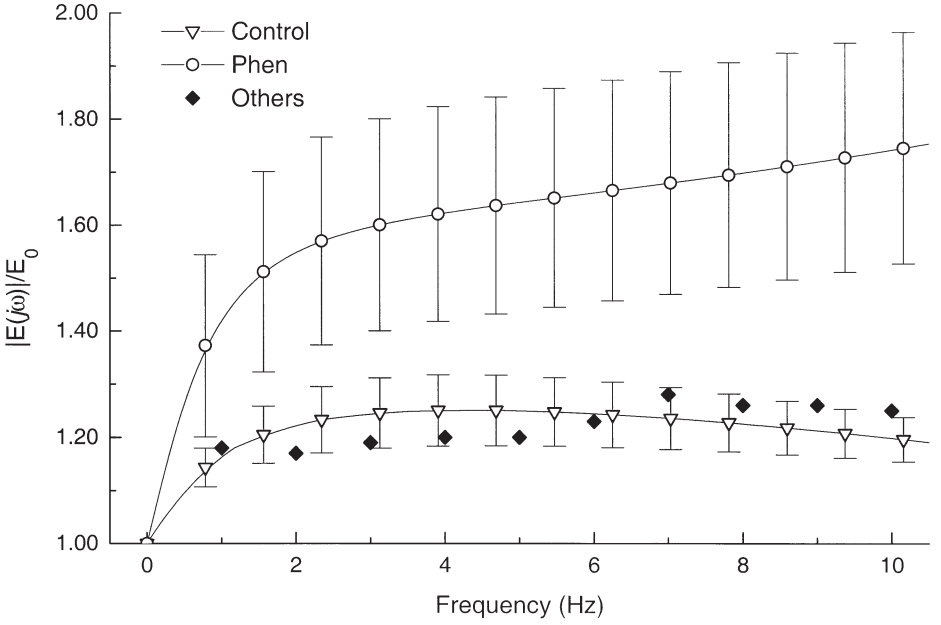

Figure 4

Dependency of the magnitude of the normalised dynamic elastic modulus during control (▽) and active (○, phenylephrine, Phen) states obtained from the entire experiment. Mean values previously obtained experimentally by Hardung (1953), Bergel (1961), Learoyd & Taylor (1966) and Tucker *et al.* (1969) are also shown(◆).

an iterative constrained procedure, where the parameters are estimated subsequently, propagating an error through the procedure, i.e. it is not a global and simultaneous optimisation procedure. From the point of view of system identification, the disadvantages are: (i) the parameters are not simultaneously estimated; (ii) it is difficult to obtain the frequency response and to explore high order models; and (iii) the method cannot be implemented with recursive on-line algorithms to track instantaneous changes in the viscoelastic properties. The results obtained in the present study allow the complete assessment of aortic wall dynamics and show reasonable agreement with those obtained in previous work (Bergel, 1961; Patel *et al.* 1969; Barra *et al.* 1993; Armentano *et al.* 1995*a*). The main advantages of the proposed approach are that the parameters are obtained simultaneously and that they can be estimated in real time. This differentiates our approach from the earlier model reported by Westerhof & Noordergraaf (1970). Furthermore, our approach provides a systematic procedure to assess the optimal number of parameters.

The first step in our work was the selection of the model structure. Several computer simulations were performed to characterise the dynamic behaviour of the arterial wall. Then, system identification (parameter estimation) was performed using an adaptive on-line algorithm and a mapping procedure to obtain the elastic, viscous and inertial moduli. Finally, model validation to predict the behaviour of the system from the estimated model was determined. We identified the constants of the constitutive equation for the aortic wall (eqn (1)) in conscious dogs characterising its mechanical properties. The linear ARX and non-linear NARX models were evaluated for this purpose. The parameters of the linear part of the NARX model presented no significant differences compared with the linear ARX model. For this reason, we will concentrate the discussion on the linear case. Time domain analysis shows that the stress–strain relationships estimated in control resting conditions and under activation of the smooth muscle were similar to the respective measured ones (Fig. 3).

Our results show a mean elastic modulus of $(0.445 \pm 0.077) \times 10^6$ Pa in control conditions. This result is comparable with that reported by Peterson *et al.* (1960) (0.53×10^6 Pa) and by Armentano *et al.* (1995*a*) (0.499×10^6 Pa) in the aorta. A significant increase of the elastic modulus was obtained during VSM activation, which modifies the elastic behaviour of the artery through the elastic contribution of the contracted muscle. The increased aortic stiffness found during activation agrees with previous reports (Cox, 1984; Barra *et al.* 1993; Armentano *et al.* 1995*a*). The highly non-linear collagen recruitment function has minor effects at the considered pressure range. In the control state, it has been demonstrated that between the onset and the

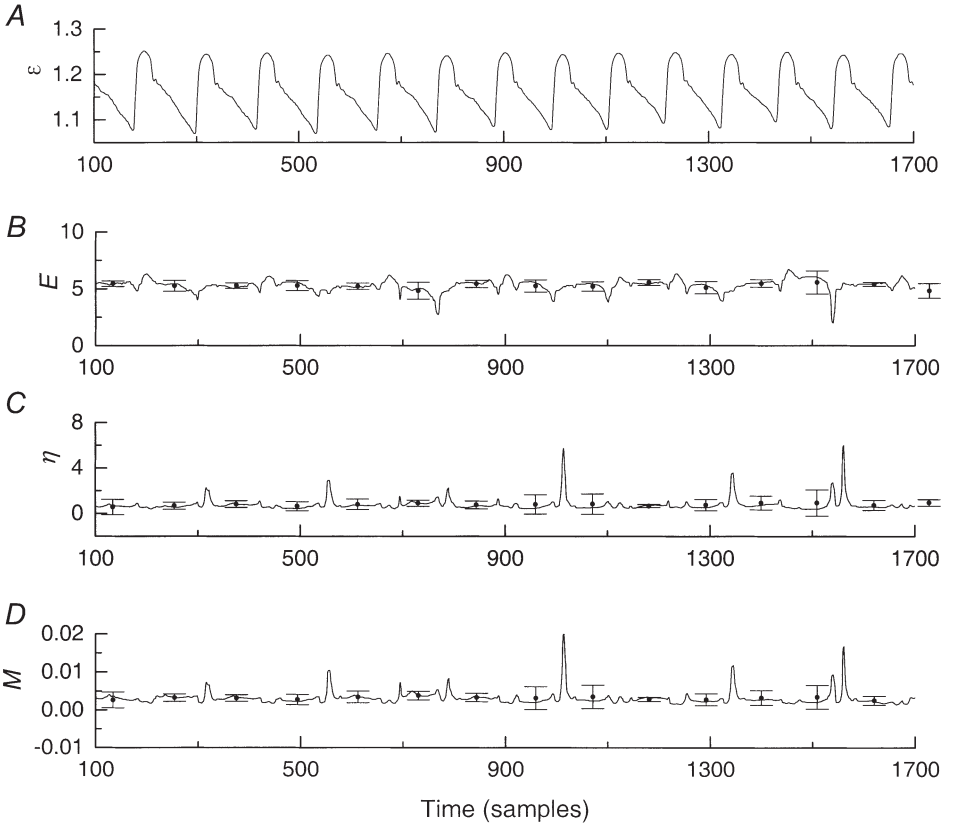

Figure 5

Time evolution of the viscoelastic parameters during control steady state and beat-to-beat mean and standard deviation of the estimated moduli. Measured strain (*A*) and elastic (*B*), viscous (*C*) and inertial (*D*) moduli (sampling frequency, 250 Hz).

end of diastole the stress–strain relationship is governed by elastin fibres (Armentano *et al.* 1995*a*). Aortic pressure at the onset of diastole is 109 ± 10 mmHg, i.e. only 15 mmHg lower than the systolic value, suggesting that basal steady state elastic behaviour can be assessed by a linear model. In effect, at this point, corresponding to 23% of the deformation level with respect to the unstressed diameter (Armentano *et al.* 1991), only 6% of the collagen fibres are recruited.

Under activation of vascular smooth muscle there was an increase in viscosity modulus, as was also reported elsewhere (Peterson *et al.* 1960; Cox, 1984; Armentano *et al.* 1995*a*). Increase in viscosity is an indirect marker of aortic smooth muscle activation (Armentano *et al.* 1995*a*) and was also found under angiotensin I converting enzyme inhibition or angiotensin II receptor blockade in conscious dogs (Barra *et al.* 1997). In humans, increases in the carotid viscosity index have been reported in hypertension (Armentano *et al.* 1995*b*).

During administration of phenylephrine, the inertial modulus was increased with respect to the control condition, which confirms the finding of Armentano *et al.* (1995*a*). This result implies that – according to the use of mass as a quantitative measure of inertia – the aortic wall mass, defined as the addition of the individual masses of each structural constituent, should also be increased under activation. It is obvious that in such conditions, factors other than the wall mass should offset the magnitude of the inertial modulus. The level of aortic pressure, the stiffness of the aortic wall and the radial acceleration of blood can codetermine this modulus. One might think that during activation the stiffness of the arterial wall could provoke a stronger link between sensors, resulting in the addition of the individual mass of sensors to the wall mass. In effect, the inertial modulus could be overestimated by the addition of the two ultrasound crystal masses and the pressure gauge.

In order to evaluate time-varying behaviour, we analysed the evolution of the parameters that mainly influence the arterial dynamics (elastic, viscous and inertial moduli) by means of the adaptive algorithm. Figure 5 shows the time evolution of the estimated (continuous line) instantaneous viscoelastic parameters and beat-to-beat mean and standard deviation (filled circles) of the parameters. Since we are not interested in the tracking properties of the algorithm, Fig. 5 does not show the characteristic transient behaviour of the adaptation process evidenced by $t = 100$ samples (0.4 s) as the initial time of the plotted values. Despite some artefacts presented in the estimation procedure, time evolution of beat-to-beat parameters shows that viscoelastic properties can be considered stationary taking into account that the analysis is carried out over stable beats. Intra-beat time evolution shows that the estimation of the elastic modulus, defined as the slope of the stress–strain relationship, presents a peak at the maximum value of strain. This result can be explained by the non-linear behaviour, due to recruitment of collagen fibres. The viscous modulus presents a transient during the maximum of the strain derivative. The inertial modulus has a similar behaviour, although in this case the inertial contribution is possibly affected by the second order derivative of strain. Further studies will be necessary to characterise the beat-to-beat variability of the mechanical properties in the conscious condition and its relationship with heart rate, pressure and diameter variability.

The cushioning function of an individual artery can be described in terms of the viscoelastic properties and not only on the basis of the pure elastic property (distensibility or compliance) (O'Rourke, 1995). The identified model provides not only the viscoelastic properties but also describes the frequency domain behaviour, i.e. the complex Young's modulus. Several authors have evaluated viscoelasticity in terms of the normalised complex Young's modulus or modulus ratio (Bergel, 1961; Learoyd & Taylor, 1966; Gow *et al.* 1974). It represents the ratio of dynamic modulus under the condition of sinusoidal forcing and linearity of the system, divided by the static modulus or by a very low frequency dynamic modulus (Learoyd & Taylor, 1966; Cox, 1984). The normalised plots are independent of the absolute values of the static modulus (or low frequency value) and allow a direct comparison with results reported by other authors and with other methods.

The hydraulic aortic filtering performance was evaluated in the frequency domain using the identified third order model ($n = m = 3$). Westerhof & Noordergraaf (1970) showed that $n = m$ is required to have bounded creep and stress relaxation. This is an important result, since a single measurement in the conscious, unsedated state was sufficient to identify all the frequency modes of the system. The results presented in Fig. 4 show a sharp increase in the low frequency range, in agreement with previous reports (Bergel, 1961; Cox, 1984). This frequency range corresponds to circulatory adjustments in cardiovascular dynamics. Then, a quite constant level is maintained between 1.5 and 10 Hz. This result is qualitatively similar to the mean data obtained in previous work (Bergel, 1961; Apter & Marquez, 1968; Cox, 1984). The results show that the magnitude of the normalised complex Young's modulus was significantly different from 1.5 to 10 Hz comparing control conditions and VSM activation. This is in accordance with previous reports (Hardung, 1953; Bergel, 1961; Learoyd & Taylor, 1966; Tucker *et al.* 1969).

In control (resting) conditions the linear model provides a fit comparable with the non-linear NARX model. Nevertheless, under high transient pressure (during exercise or stress) the non-linear model should be considered to improve the fitting performance. Using the proposed method, the elastic, viscous and inertial moduli could be evaluated in a single beat. The assessment of mechanical properties in humans using non-invasive techniques (e.g. ultrasound or tonometry) is a growing field in clinical applications (Armentano, 1995*b*; Reneman & Hoeks, 2000). Further studies should consider non-invasive techniques using the single beat modelling approach to estimate the arterial dynamic properties.

Arterial wall dynamics were modelled based on the stress–strain relationship in conscious dogs. General linear ARX models and non-linear NARX structures for modelling the arterial wall dynamics are presented. The linear ARX model provides a direct physical insight of the arterial wall.

Mechanical parameters were obtained and the effect of vascular smooth muscle activation could be summarised as increases in the viscous, elastic and inertial wall moduli. We derived these parameters using a real time recursive algorithm. The identified model not only provides a temporal description but also the frequency domain response of the arterial wall dynamics in the conscious state. The results obtained in this work demonstrate that the frequency dependence of the aortic wall dynamics, using a parametric system identification approach, is affected during vascular smooth muscle activation.

APPENDIX

Linear and semi-physical structures

The linear parametric ARX model is described by

$$\hat{y}(t) = -\sum_{j=1}^{n_y} a_j y(t-j) + \sum_{i=1}^{n_x} b_i x(t-i) + v(t), \qquad \text{(A1)}$$

where n_y and n_x define the order of the model and $\hat{y}(t)$ is the estimated output (strain) and $x(t)$ is the input (stress), $v(t)$ is a perturbation considered typically as noise, or the term that cannot be assessed by the model (Ljung, 1999). The ARX model can be described by

$$\hat{y}(t) = \phi^T \hat{\theta}(t) + v(t), \qquad \text{(A2)}$$

where $\phi(t) = [-y(t-1) \quad -y(t-2) \ldots -y(t-n_y) \quad x(t-1) \; x(t-2) \ldots x(t-n_x)]^T$ is the input vector and $\theta = [a_1 \, a_2 \ldots a_{n_y} \; b_1 \; b_2 \ldots b_{n_x}]^T$ is the parameter vector to be estimated on the basis that $y(t)$ and $\phi(t)$ for $t = 1, \ldots, N$ are known. It is important to notice that the parameters from (eqn (1)) can be related to the ARX parameters through a complex mapping. The inverse bilinear mapping from the z to s plane was used to reach this task (Lam, 1980).

The non-linear behaviour of the pure elastic components (elastic, collagen fibres and VSM) was considered by the following stress–strain relationship:

$$\sigma = E\epsilon + \alpha\epsilon^2 + \beta\epsilon^3. \qquad \text{(A3)}$$

The selection of this model presents the advantage that it can be easily incorporated into the dynamic model identification framework presented previously.

One of the problems in grey box identification is the regressor selection procedure. Using *a priori* information (eqn (A3)) about the system, the following bilinear model is proposed:

$$\hat{y}(t) = -\sum_{i=1}^{n_y} a_i y(t-i) + \sum_{j=1}^{n_x} b_j x(t-j) + \sum_{k=2}^{3} c_{k-1} y(t-1)^k + v(t), \qquad \text{(A4)}$$

where the linear part (see eqn (A1)) is preserved and the parameters $\{c_k, \; k = 2, \; 3\}$ are to be related to α and β, respectively.

Model order selection and parameter estimation

In this study, the optimal order model was the one that minimised the Akaike information criterion (Akaike, 1969) defined by the equation

$$\mathrm{AIC}(N_\mathrm{p}) = N \ln(\sigma_\epsilon^2) + 2N_\mathrm{p}, \qquad \text{(A5)}$$

where N_p is the number of parameters, N is the number of data samples and σ_ϵ^2 is the residual variance defined by

$$\sigma_\epsilon^2 = \frac{1}{N-1-d} \sum_{t=\mathrm{d}+1}^{N} e(t)^2, \qquad \text{(A6)}$$

where $e(t) = y(t) - \hat{y}(t)$ is the prediction error and $d = \max\{n_x, n_y\}$. Other criteria can be considered but the AIC is a good compromise between the number of parameters and the residual variance (Ljung, 1999).

A natural way for estimating $\theta(t)$ is minimising what the model cannot represent. The cost function to be minimised is usually of the form

$$J(\theta) = \sum_{t=1}^{N} \alpha^t (y(t) - \phi^T \hat{\theta}(t))^2. \qquad \text{(A7)}$$

This function can be minimised iteratively and tracking time-varying systems. In this paper we use the recursive least-squares algorithm that can be summarised by the following equations (Ljung, 1999):

$$\theta(t) = \theta(t-1) + L(t)\epsilon(t),$$

$$\epsilon(t) = y(t) - \phi^T(t)\hat{\theta}(t-1),$$

$$L(t) = \frac{P(t-1)\phi(t)}{\lambda(t) + \phi^T(t)P(t-1)\phi(t)},$$

$$P(t) = \frac{P(t-1) - \dfrac{P(t-1)\phi(t)\phi^T(t)P(t-1)}{\lambda(t) + \phi^T(t)P(t-1)\phi(t)}}{\lambda(t)}, \qquad \text{(A8)}$$

where $\theta(t) \in \Re^{n \times 1}$ is the estimated parameter vector, $n = N_\mathrm{p}$ is the number of parameters, $\lambda(t)$ is the forgetting factor, $P(t) \in \Re^{n \times 1}$ is the covariance matrix and $L(t) \in \Re^{n \times n}$ is the gain matrix. If we assume that the model represents the arterial wall dynamics, the algorithm is consistent if the input is sufficiently rich and has the property of persistency of excitation, or, equivalently, if it excites all modes of the system (Ljung, 1999). Initial conditions for $\theta(0)$ and $P(0)$ can be set using previous knowledge about the system. Initial values of $\theta(0) = 0$ and $P(0) = kI$, where I is the identity matrix and k is a constant with typical values of 10 or 100, were considered in this study.

Akaike, H. (1969). Fitting autoregressive models for prediction. *Annals of the Institute of Statistical Mathematics* **21**, 243–247.

Apter, J. & Marquez, E. (1968). Correlation of visco-elastic properties of large arteries with microscopic structures. *Circulation Research* **12**, 393–404.

Armentano, R., Barra, J., Levenson J., Simon, A. & Pichel, R. (1995*a*). Arterial wall mechanics in conscious dogs. *Circulation Research* **76**, 468–478.

Armentano, R., Levenson, J., Barra, J., Cabrera Fischer, E., Breitbart, G., Pichel, R. & Simon, A. (1991). Assessment of elastin and collagen contribution to aortic elasticity in conscious dogs. *American Journal of Physiology* **260**, H1870–1877.

Armentano, R., Megnien, J., Simon, A., Bellenfant, F., Barra, J. & Levenson, J. (1995*b*). Effects of hypertension on viscoelastic properties of common carotid and femoral arteries in humans. *Hypertension* **26**, 48–54.

Barra, J., Armentano, R., Levenson, J., Cabrera Fischer, E., Pichel, R. & Simon, A. (1993). Assessment of smooth muscle contribution to descending thoracic aortic elastic mechanics in conscious dogs. *Circulation Research* **73**, 1040–1050.

Barra, J., Levenson, J., Armentano, R., Cabrera Fischer, E., Pichel, R. & Simon, A. (1997). In vivo angiotensin II receptor blockade and converting enzyme inhibition on canine aortic viscoelasticity. *American Journal of Physiology* **272**, H859–868.

Bauer, R. D. (1984). Rheological approaches of arteries. *Biorheology* **1**, 159–167.

Bergel, D. (1961). The static properties of the arterial wall. *Journal of Physiology* **156**, 458–469.

Cabrera Fischer, E., Armentano, R., Levenson, J., Barra, J., Morales, M., Breitbart, G., Pichel, R. & Simon, A. (1991). Paradoxically decreased aortic wall stiffness in response to vitamin D3-induced calcinosis: a biphasic analysis of segmental elastic properties in conscious dogs. *Circulation Research* **68**, 1549–1559.

Christensen, R. M. (1971). *Theory of Viscoelasticity, an Introduction*. Academic Press, New York and London.

Cox, R. H. (1984). Viscoelastic properties of canine pulmonary arteries. *American Journal of Physiology* **15**, H90–96.

Davies P. F. (1995). Flow-mediated endothelial mechano-transduction. *Physiological Reviews* **75**, 519–560.

Dobrin, P. (1984). Mechanical behaviour of vascular smooth muscle in cylindrical segments of arteries in vitro. *Annals of Biomedical Engineering* **12**, 497–510.

Dobrin, P. & Rovick, A. (1969). Influence of vascular smooth muscle on contractile mechanisms and elasticity of arteries. *American Journal of Physiology* **217**, 1644–1651.Fung, Y. C. (1981). *Biomechanics. Mechanical Properties of Living Tissues*. Springer-Verlag, New York.

Goedhard, W., Knoop, A. & Westerhof, N. (1973). The influence of vascular smooth muscle contraction on elastic properties of pig's thoracic aorta. *Acta Cardiologica* **28**, 415–430.

Gow, B., Schonfeld, D. & Patel, D. J. (1974). The dynamic elastic properties of the canine left circumflex coronary artery. *Journal of Biomechanics* **7**, 389–395.

Gow, B. & Taylor, M. (1968). Measurement of viscoelastic properties of arteries in the living dog. *Circulation Research* **13**, 111–122.

Hardung, V. (1953). Vergleichende Messungen der dynamischen Elastizitat und Viskositat von Blutgeffasen, Kaustschuk und synthetischen Elastomeren. *Helvetica Physiologica Acta* **11**, 194–211.

Hardung, V. (1970). Dinamische Elastizitat und innere Reibung muskularer Blutgefable bei verschiedener durch Dehnung und tonische Contraktion hervorgerufener Wandspannung. *Archiv fur Kreislaufforschung* **61**, 83–100.

Hayashi, K. (1993). Experimental approaches on measuring the mechanical properties and constitutive laws of arterial walls. *Journal of Biomechanical Engineering* **115**, 481–488.

Lam, H. Y. (1980). *Analog and Digital Filters: Design and Realization*. Prentice Hall, Englewood Cliffs, New Jersey.

Langewouters, G. J., Wesseling, K. H., Goedhard, W. J. (1984). The static elastic properties of 45 human thoracic and 20 abdominal aortas in vitro and the parameters of a new model. *Journal of Biomechanics* **17**, 425–435.

Learoyd, B. & Taylor, M. (1966). Alterations with age in the viscoelastic properties of human arterial wall. *Circulation Research* **18**, 218.

Ljung, L. (1999). *System Identification. Theory for the User*, 2nd edn. PTR Prentice Hall, Upper Saddle River, NJ, USA.

Milnor, W. K. (1982). *Hemodynamics*. Williams & Wilkins Co, Baltimore.

Nichols, W. W. & O'Rourke, M. F. (1990). *McDonald's Blood Flow in Arteries*. Edward Arnold Publishers Ltd, London.

O'Rourke, M. F. (1995). Second workshop on structure and function of large arteries: Part I. Mechanical principles in arterial disease. *Hypertension* **26**, 2–9.

Pagani, M., Baig, H., Sherman, A., Manders, W., Quinn, P., Patrick, T., Franklin, D. & Vatner, S. (1979). Measurement of multiple simultaneous small dimensions and study of arterial pressure–dimension relations in conscious animals. *American Journal of Physiology* **235**, H610–617.

Patel, D., Janicki, J. & Carew, T. (1969). Static anisotropic elastic properties of the aorta in living dogs. *Circulation Research* **25**, 765–769.

Peterson, L., Jensen, R. & Parnell, J. (1960). Mechanical properties of arteries in vivo. *Circulation Research* **8**, 622–639.

Reneman, R. S. & Hoeks, A. P. (2000). Noninvasive vascular ultrasound: an asset in vascular medicine. *Cardiovascular Research* **45**, 27–35.

Simon, A., O'Rourke, M. F. & Levenson, J. (1991). Arterial distensibility and its effect on wave reflection and cardiac loading in cardiovascular disease. *Coronary Artery Disease* **2**, 1111–1120.

Sipkema, P. (1979). Low-frequency viscoelastic properties of canine femoral artery in vivo. *American Journal of Physiology* **236**, H720–724.

Sugeno, M. & Kang, G. (1988). Structure identification of fuzzy model. *Fuzzy Sets and Systems* **26**, 15–33.

Tucker, W. K., Janicki, J., Plowman, F. & Patel, D. (1969). A device to test mechanical properties of tissues and transducers. *Journal of Applied Physiology* **26**, 656–658.

Vatner, S., Pasipoularides, A. & Mirsky, I. (1984). Measurement of arterial pressure–dimension relationships in conscious animals. *Annals of Biomedical Engineering* **12**, 521–534.

Westerhof, N. & Noordergraaf, A. (1970). Arterial viscoelasticity: a generalized model. Effect on input impedance and wave travel in the systematic tree. *Journal of Biomechanics* **3**, 357–379.

Wuyts, F. L., Vanhuyse, V., Langewouters, G., Decraemer, W., Raman, E. & Buyle, S. (1995). Elastic properties of human aortas in relation to age and atherosclerosis: a structural model. *Physics in Medicine and Biology* **40**, 1577–1597.

Acknowledgements

The authors wish to thank the program SECYT-ECOS (project no. A97S03) and INSERM (CRI 9610) for partial financial support. They would also like to thank Dr Alberto Crottogini for his help with preparing the manuscript.